

Concurrent duplication of the *Cid* and *Cenp-C* genes in the *Drosophila* subgenus with signatures of subfunctionalization and male germline-biased expression

José R. Teixeira¹, Guilherme B. Dias¹, Marta Svartman¹, Alfredo Ruiz², Gustavo C. S. Kuhn¹

¹Departamento de Biologia Geral, Universidade Federal de Minas Gerais, Belo Horizonte, Minas Gerais, Brazil, Postal Code: 31270-901

²Departament de Genètica i de Microbiologia, Universitat Autònoma de Barcelona, Bellaterra (Barcelona), Spain, Postal Code: 08193

Corresponding author:

Prof. Dr. Gustavo C. S. Kuhn

Laboratório de Citogenômica Evolutiva, Departamento de Biologia Geral, Instituto de Ciências Biológicas, Universidade Federal de Minas Gerais, Av. Antônio Carlos 6627 – Pampulha, Belo Horizonte, MG, Brazil. Postal Code: 31270-901.

Fone: +55 (31) 3409-3062

E-mail: gcskuhn@ufmg.br

Running title: *Cid* and *Cenp-C* duplication in *Drosophila*

1 **Abstract**

2

3 Despite their essential role in the process of chromosome segregation in eukaryotes, kinetochore
4 proteins are highly diverse across species, being lost, duplicated, created, or diversified during
5 evolution. Based on comparative genomics, the duplication of the inner kinetochore proteins CenH3
6 and Cenp-C, which are interdependent in their roles of establishing centromere identity and function,
7 can be said to be rare in animals. Surprisingly, the *Drosophila* CenH3 homolog *Cid* underwent four
8 independent duplication events during evolution. Particularly interesting are the highly diverged and
9 subfunctionalized *Cid1* and *Cid5* paralogs of the *Drosophila* subgenus, which show that over one
10 thousand *Drosophila* species may encode two *Cid* genes, making those with a single copy a minority.
11 Given that CenH3 and Cenp-C likely co-evolve as a functional unit, we investigated the molecular
12 evolution of *Cenp-C* in species of *Drosophila*. We report yet another *Cid* duplication within the
13 *Drosophila* subgenus and show that not only *Cid*, but also *Cenp-C* is duplicated in the entire
14 subgenus. The *Cenp-C* paralogs, which we named *Cenp-C1* and *Cenp-C2*, are highly divergent. The
15 retention of key motifs involved in centromere localization and function by both Cenp-C1 and Cenp-
16 C2 makes neofunctionalization unlikely. In contrast, the alternate conservation of some functional
17 motifs between the proteins is indicative of subfunctionalization. Interestingly, both *Cid5* and *Cenp-*
18 *C2* are male germline-biased and evolved adaptively. Our findings point towards a specific inner
19 kinetochore composition in a specific context (i.e., spermatogenesis), which could prove valuable for
20 the understanding of how the extensive kinetochore diversity is related to essential cellular functions.

21

22 **Keywords:** CenH3, Cenp-C, gene duplication, centromere, kinetochore, *Drosophila*

23 **Introduction**

24

25 During eukaryotic cell division, accurate chromosome segregation requires the interaction of
26 chromosomes with the microtubules from the spindle apparatus. This interaction is mediated by the
27 kinetochore, a multiprotein structure that is hierarchically assembled onto centromeres. Upstream in
28 the assembly of the kinetochore are CenH3 and Cenp-C, two interdependent proteins in their roles of
29 establishing centromere identity and function. CenH3 is the histone H3 variant found in centromeric
30 nucleosomes and, therefore, considered the centromere epigenetic marker (Dalal *et al.* 2007). During
31 kinetochore assembly, Cenp-C binds to CenH3 and recruits other kinetochore proteins (Przewloka *et al.*
32 *et al.* 2011; Liu *et al.* 2016). CenH3 and Cenp-C are fundamentally interdependent because the
33 centromeric localization of one depends on the centromeric localization of the other (Erhardt *et al.*
34 2008; Orr and Sunkel 2011). This interdependence is also illustrated by the fact that both CenH3 and
35 Cenp-C have similar phylogenetic profiles (i.e., they have similar patterns of presence and absence
36 across the eukaryotic evolutionary tree) and likely co-evolve as a functional unit (van Hooff *et al.*
37 2017). One interesting case is that seen in insects, where CenH3 was lost independently five times,
38 and in all these cases Cenp-C was also lost (Drinnenberg *et al.* 2014).

39 Despite the essentiality of centromeres, both centromeric DNA (CenDNA) and proteins are
40 remarkably diverse (Henikoff *et al.* 2000; Talbert *et al.* 2004; Plohl *et al.* 2008). This rapid evolution
41 despite the expectation of constraint is referred to as the “centromere paradox” (Henikoff *et al.* 2001).
42 This paradox may be explained by the centromere drive hypothesis, which proposes that genetic
43 conflicts during female meiosis drive centromere evolution (Henikoff *et al.* 2001; Dawe and Henikoff
44 2006).

45 In the female meiosis of animals and plants, the meiotic spindle fibers are asymmetric in a way
46 that one pole will originate a polar body and the other will give rise to the oocyte. As a result, there
47 is potential for non-mendelian (biased) inheritance if a pair of homologous chromosomes have
48 kinetochores that interact unequally with the spindle fibers (Ross and Malik 2014). The heterogeneity
49 in kinetochore function between homologs is a result of differences in abundance of centromeric
50 DNA sequences. One homolog may have a ‘strong’ centromere, which has an expanded cenDNA that
51 recruits more kinetochore proteins and delivers its chromosome into the oocyte at > 50% frequency,
52 or a ‘weak’ centromere, which has a contracted cenDNA that in turn recruits less kinetochore proteins
53 and delivers its chromosome into the oocyte at < 50% frequency (Iwata-Otsubo *et al.* 2017). However,
54 the spread of expanding centromeres throughout a population might be accompanied by deleterious
55 effects, such as increased male sterility or a skewed sex ratio (Fishman and Saunders 2008;
56 Rutkowska and Badyaev 2008; Malik and Henikoff 2009). The centromere drive hypothesis proposes
57 that changes in CenH3 and Cenp-C related to more ‘flexible’ DNA-binding preferences are expected

58 to counteract the transmission advantage gained by expanded centromeres and diminish the
59 associated deleterious effects, thus restoring meiotic parity for both homologs (Henikoff et al. 2001;
60 Dawe and Henikoff 2006).

61 The kinetochore is highly diverse across species, with proteins being lost, duplicated, created, or
62 diversified during evolution (van Hooff *et al.* 2017). Given that data directly supporting a correlation
63 between the evolution of cenDNA, CenH3 and Cenp-C are still absent, it is not known if and how
64 such structural divergence is related to centromere drive suppression. However, the
65 subfunctionalization of *CenH3* paralogs in some lineages of *Drosophila* has been hypothesized to be
66 linked to centromere drive suppression. Kursel and Malik (2017) have recently reported that the
67 *Drosophila* *CenH3* homolog *Cid* underwent four independent duplication events during evolution,
68 and some *Cid* paralogs are primarily expressed in the male germline and evolve under positive
69 selection (Kursel and Malik 2017). These duplications could have allowed the rapid evolution of
70 centromeric proteins without compromising their essential function by separating functions with
71 divergent fitness optima. The existence of germline-biased *CenH3* duplicates (which do not interfere
72 with essential mitotic functions) in genetically tractable organisms provides an opportunity to study
73 the functional consequences of the genetic variation for kinetochore-related processes.

74 Given the interdependence between CenH3 and Cenp-C, we decided to further analyze the
75 molecular evolution of the *Cid* and *Cenp-C* genes in *Drosophila* species. Here, we report a novel *Cid*
76 duplication within the *Drosophila* subgenus and show that not only *Cid*, but also *Cenp-C* is duplicated
77 in the entire *Drosophila* subgenus. The *Cid* and *Cenp-C* paralogs likely subfunctionalized, as some
78 motifs are alternatively conserved between the paralogs. Interestingly, both the *Cid* and *Cenp-C*
79 duplications generated copies that are male-biased and evolve under positive selection. Our findings
80 point towards a specific kinetochore composition in a specific context (i.e., the male germline), which
81 could prove valuable for the understanding of how the extensive kinetochore diversity is related to
82 essential cellular functions.

83

84 **Results and Discussion**

85

86 ***Cid1* was replaced by a new paralog in a clade within the *Drosophila* subgenus**

87

88 Duplicate *Cid* genes exist in *D. eugracilis* (*Cid1*, *Cid2*) and in the *D. montium* subgroup (*Cid1*,
89 *Cid3*, *Cid4*), both within the *Sophophora* subgenus, and in the entire *Drosophila* subgenus (*Cid1*,
90 *Cid5*). In all analyzed species from the *Drosophila* subgenus, *Cid1* is flanked by the *cbc* and *bbc*
91 genes, and *Cid5* is flanked by the *Kr* and *CG6907* genes (Kursel and Malik 2017). As expected, we
92 found two *Cid* genes while looking for the orthologs of *Cid1* and *Cid5* in the assembled genomes of

93 two cactophilic species from the *Drosophila* subgenus, *D. buzzatii* and *D. seriema* (*repleta* group).
94 Surprisingly, while one of the genes is present in the expected locus of *Cid5*, the other one is located
95 in an entirely different locus, flanked by the *CG14341* and *IntS14* genes. We named this new paralog
96 as *Cid6*.

97 By investigating the *Cid1* locus of *D. buzzatii*, we found a myriad of transposable elements (TEs)
98 surrounding a 116-bp fragment of the original *Cid1* gene (fig. 1, upper panel). Due to fragmentary
99 genome assembly, the *Cid1* locus of *D. seriema* could not be identified. Both *Cid5* and *Cid6* of *D.*
100 *buzzatii* and *D. seriema* share ~40% amino acid identity but, in contrast, *Cid6* of each species and
101 *Cid1* of the closely related *D. mojavensis* are much more similar, sharing ~80% identity. Fluorescent
102 *in situ* hybridizations on polytene chromosomes showed that *Cid6* is distal (in relation to the
103 chromocenter) in the Muller element B of *D. buzzatii* and *D. seriema*, and that *Cid1* is proximal in
104 the Muller element C of *D. mojavensis* and the outgroup *D. virilis* (fig. 1, lower panel). Therefore,
105 we inferred that *Cid1* was degenerated by several TE insertions after the origin of *Cid6* by an inter-
106 chromosomal duplication of *Cid1* in the lineage that gave rise to *D. buzzatii* and *D. seriema*. The time
107 of divergence between *D. buzzatii* and *D. seriema* has been estimated at ~4.6 mya, and the divergence
108 between them and the closely related *D. mojavensis* has been estimated at ~11.3 mya (Oliveira *et al.*
109 2012). Therefore, the *Cid1* duplication that gave rise to *Cid6* happened between ~4.6 and 11.3 mya.

110 Why *Cid6* remained while *Cid1* degenerated? The *Cid1* locus of *D. buzzatii* is located in the most
111 proximal region of the Muller element C (scaffold 115; Guillén *et al.* 2014), which is very close to
112 the pericentromeric heterochromatin where TEs are highly abundant (Pimpinelli *et al.* 1995; Casals
113 *et al.* 2005; Rius *et al.* 2016). Natural selection is known to be less effective in pericentromeric and
114 adjacent regions due to low rates of crossing-over (Zhang and Kishino 2004; Clément *et al.* 2006;
115 Comeron *et al.* 2012; Nambiar and Smith 2016). Thus, it is reasonable to suggest that the presence of
116 an extra copy of *Cid1* (i.e., *Cid6*) in Muller element B alleviated the selective pressure on *Cid1* in
117 Muller element C, whose proximity to the pericentromeric heterochromatin fostered its degradation
118 by several posterior TE insertions.

119

120 ***Cenp-C* is duplicated in the *Drosophila* subgenus**

121

122 It has been recently shown that the *Drosophila* *CenH3* homolog *Cid* underwent duplication
123 events during evolution (Kursel and Malik, 2017). Given that CenH3 and Cenp-C are interdependent
124 and coevolve as a functional unit, we investigated if *Cenp-C* was also duplicated in *Drosophila*
125 species where *Cid* was duplicated.

126 In *D. eugracilis*, in species from the *montium* subgroup, and in all the other species of the
127 *Sophophora* subgenus we found only one copy of *Cenp-C*, which is always flanked by the *5-HT2B*

128 gene. On the other hand, in the species of the *Drosophila* subgenus we found two copies of *Cenp-C*
129 with ~52% nucleotide identity, which we named *Cenp-C1* and *Cenp-C2*: the former is flanked by the
130 *5-HT2B* and *CG1427* genes, and the latter is flanked by the *CLS* and *RpL27* genes. A maximum
131 likelihood tree showed that *Cenp-C* was likely duplicated after the split between the *Sophophora* and
132 *Drosophila* subgenera but before the split between *D. busckii* and the other species of the *Drosophila*
133 subgenus (fig. 2). Thus, we concluded that *Cenp-C2* originated from a duplication of *Cenp-C1* in the
134 lineage that gave rise to species of the *Drosophila* subgenus, at least 50 mya (Russo *et al.* 2013).

135 Why *Cenp-C* is duplicated only in the *Drosophila* subgenus if *Cid* is also duplicated in *D.*
136 *eugracilis* and in the *montium* subgroup? The fact that both *Cid* and *Cenp-C* duplicated in the
137 *Drosophila* subgenus does not mean that there is a cause-and-effect relationship between the
138 duplications. However, it probably means that the new paralogs influenced each other's evolution.
139 As a histone H3 variant, CenH3 has the C-terminal histone fold domain, which is reasonably
140 conserved among species, and the N-terminal tail (NTT), which is highly variable among species
141 (Henikoff *et al.* 2000). The NTT evolves in a modular manner, with four core motifs always
142 conserved when there is only one *Cid* protein encoded in the genome (Kursel and Malik 2017). In *D.*
143 *eugracilis*, the *Cid2* paralog functionally replaced the pseudogenized ancestral *Cid1* paralog. In
144 species of the *montium* subgroup, these four motifs are alternated between the paralogs, which share
145 ~25% amino acid identity. In contrast, in species of the *Drosophila* subgenus, all four motifs are
146 conserved in *Cid1* but only 1-2 are conserved in *Cid5*, with the paralogs sharing only ~15% amino
147 acid identity at their NTT. Therefore, we propose that if the NTT of *Cid* interacts with *Cenp-C*, a new
148 *Cenp-C* copy would allow a higher divergence of the *Cid* paralogs by alleviating the selective pressure
149 over the *Cid/Cenp-C* interaction, thus explaining the higher divergence of the *Cid1* and *Cid5* paralogs.
150 However, future studies focusing on the specific interactions between *Cid* and *Cenp-C* shall shed
151 light on the exact basis behind the flexibility of these two proteins during evolution.

152

153 **Some Cenp-C motifs are alternatively conserved between Cenp-C1 and Cenp-C2** 154

155 *Cenp-C* was previously thought to be absent in *Drosophila* (Talbert *et al.* 2004), but it turned out
156 that a protein that interacts with the regulatory subunits of separase is a highly divergent *Cenp-C*
157 homolog (Heeger *et al.* 2005). The *D. melanogaster* *Cenp-C1*, as characterized by Heeger *et al.*
158 (2005), has seven independent functional motifs, from N- to C-terminal: arginine-rich (R-rich),
159 drosophilids *Cenp-C* homology (DH), AT hook 1 (AT1), nuclear localization signal (NLS), CenH3
160 binding (also known as the *Cenp-C* motif), AT hook 2 (AT2), and C-terminal dimerization (Cupin).
161 The R-rich and DH motifs, as well as both AT1 and AT2 motifs (which may mediate binding to the
162 minor groove of DNA), are functionally poorly characterized. However, all except AT1 appear to hold

163 essential functions, as Cenp-C1 variants lacking these regions are unable to prevent phenotypic
164 abnormalities in *Cenp-C1* mutant embryos (Heeger *et al.* 2005). In fact, it is known that the DH motif
165 must be involved in the recruitment of kinetochore proteins (Przewloka *et al.* 2011; Liu *et al.* 2016).
166 Furthermore, arginine 1101 (R1101), present in the CenH3 binding motif, is crucial for centromere
167 localization (Heeger *et al.* 2005). Given the functional relevance of these motifs, we searched for
168 them in both Cenp-C1 and Cenp-C2.

169 With the exception of *D. kikkawai* (from the *montium* subgroup), in which the AT2 motif is
170 absent, all seven motifs are conserved in Cenp-C1 from all other species of the *Sophophora* subgenus.
171 In contrast, the motifs are alternatively conserved between Cenp-C1 and Cenp-C2 in species from the
172 *Drosophila* subgenus (fig. 3). Both Cenp-C1 and Cenp-C2 of all species have the DH, NLS, and
173 CenH3 binding motifs (with the corresponding R1101 of *D. melanogaster*), but lack the AT1 motif.
174 Furthermore, only Cenp-C2 has the R-rich and AT2 motifs conserved. Both Cenp-C1 and Cenp-C2
175 of most species have the Cupin motif, the exceptions being Cenp-C1 of *D. busckii*, which lacks the
176 final half of it, and Cenp-C2 of *D. grimshawi*, which entirely lacks it. Interestingly, the DH and NLS
177 motifs of Cenp-C2 are more similar to those of *Sophophora* Cenp-C1 than to those of *Drosophila*
178 Cenp-C1 (table 1). For the logo representation of the motifs, see Supplementary Figure S1.

179 The conservation of the DH motif (involved in the recruitment of kinetochore proteins) and the
180 NLS and CenH3 binding motifs (involved in centromere localization) in both Cenp-C1 and Cenp-C2
181 (fig. 3) indicates that it is unlikely that any of the paralogs underwent neofunctionalization. The
182 (partial) loss of the Cupin motif in *D. busckii* and *D. grimshawi* points towards subfunctionalization.
183 It is currently difficult to evaluate the loss of the AT1 motif in both Cenp-C1 and Cenp-C2, given that
184 its function is unknown. However, the higher similarity of the DH and NLS motifs of Cenp-C2 to
185 those of *Sophophora* Cenp-C1, the loss of the R-rich and AT2 motifs in Cenp-C1, and their retention
186 in Cenp-C2 are highly indicative of subfunctionalization.

187

188 **The *Cenp-C* paralogs are differentially expressed**

189

190 Given that Cenp-C is incorporated onto centromeres concomitantly with Cid (Schuh *et al.* 2007)
191 and that the excess of both proteins can cause centromere expansion and kinetochore failure
192 (Schittenhelm *et al.* 2010), the expression of both proteins needs to be tightly regulated. Kursel and
193 Malik (2017) showed that *Cid5* expression is male germline-biased and proposed that *Cid1* and *Cid5*
194 subfunctionalized and now performed nonredundant centromeric roles. In order to investigate if *Cenp-*
195 *C1* and *Cenp-C2* are differentially expressed and correlated in some way with the expression of the
196 *Cid* paralogs, we analyzed the available transcriptomes from embryos, larvae, pupae and adult

197 females and males of *D. buzzatii* (Guillén *et al.* 2014), and from testes of *D. virilis* and *D. americana*
198 (BioProject Accession PRJNA376405).

199 While *Cid6* is transcribed in all stages of development in *D. buzzatii*, confirming that *Cid6*
200 functionally replaced *Cid1*, *Cid5* transcription is limited to pupae and adult males, with a higher
201 transcription than *Cid6* in the latter (fig. 4A). Additionally, *Cid5* transcription is elevated in testes of
202 *D. virilis* and *D. americana*, whereas *Cid1* is virtually silent (fig. 4C). Our results further support the
203 finding of Kursel and Malik (2017) that *Cid5* displays a male germline-biased expression. In this
204 context, our finding that *Cid5* is also transcribed in pupae of *D. buzzatii* may be related to the ongoing
205 development of the male gonads.

206 In contrast to the *Cid* paralogs, we found that both *Cenp-C1* and *Cenp-C2* are transcribed in
207 almost all stages of *D. buzzatii* development, with the exception of larvae (fig. 4B). *Cenp-C1*
208 transcription is higher than that of *Cenp-C2* in *D. buzzatii* embryos and adult females. On the other
209 hand, transcription of *Cenp-C2* is higher than that of *Cenp-C1* in *D. buzzatii* pupae and adult males.
210 *Cenp-C2* transcription is also higher than that of *Cenp-C1* in *D. virilis* testes, but there is no significant
211 difference between their expression in *D. americana* testes (fig. 4D). Therefore, similarly to the
212 findings for the *Cid* paralogs, the differential expression between the *Cenp-C* paralogs in testis
213 supports the subfunctionalization hypothesis. The male germline-biased expression of both *Cid5* and
214 *Cenp-C2* points towards their interaction in spermatogenesis, but biochemical assays need to be
215 performed to confirm this possible interdependence.

216

217 **The *Cid* and *Cenp-C* paralogs show signs of positive selection in species of the** 218 ***repleta* group**

219

220 The centromere drive hypothesis states that CenH3 and Cenp-C constantly evolve in an effort to
221 suppress and diminish the associated deleterious effects of cenDNA selfish spread throughout the
222 population by female meiotic drive (Henikoff *et al.* 2001; Dawe and Henikoff 2006). However, it has
223 been proposed that the rapid evolution of CenH3 required for the “drive suppressor” function may be
224 disadvantageous for canonical functions (e.g., mitosis; Finseth *et al.* 2015; Kursel and Malik 2017).
225 The possibility that the paralogs achieved fitness optima for divergent functions predicts that selection
226 may act differently in each of the *Cid* and *Cenp-C* paralogs. To test this hypothesis, we looked in our
227 full-length alignments of the *Cid* and *Cenp-C* paralogs for signatures of positive selection using
228 maximum likelihood methods. Given that CenH3 and Cenp-C are highly divergent, we focused our
229 analyses on five closely related cactophilic *Drosophila* species from the *repleta* group (*D. mojavensis*,
230 *D. arizonae*, *D. navojoa*, *D. buzzatii* and *D. seriema*).

231 We first used random-site and branch-site models to test for positive selection on particular sites
232 during the evolution of the paralogs. The random-site models, which allow ω to vary among sites but
233 not across lineages, revealed that both *Cid5* and *Cenp-C2* show extensive signs of positive selection
234 (table 2). Particularly, Bayes Empirical Bayes analyses identified with a posterior probability > 95%
235 four amino acids in the NTT of *Cid5* and six amino acids across *Cenp-C2* as having evolved under
236 positive selection. Of the six *Cenp-C2* amino acids, one is in the DH motif, one is in the Cupin motif,
237 and the remaining four are in inter-motif sequences.

238 The branch-site models allow ω to vary both among sites and across branches on the tree and aim
239 to detect positive selection affecting a few sites along particular lineages. The tests revealed that the
240 paralogs show signs of positive selection in the branches of *D. navojoa Cid1* and *Cenp-C2*, *D. buzzatii*
241 *Cenp-C1* and *Cenp-C2*, and *D. seriema Cenp-C1* and *Cenp-C2* (table 3). Particularly, Bayes
242 Empirical Bayes analyses identified with posterior probability > 60% four amino acids in the NTT of
243 *D. navojoa Cid1*, seven in inter-motif sequences of *D. navojoa Cenp-C2*, four in *D. buzzatii Cenp-*
244 *C1* (one in the DH motif and three in inter-motif sequences), six in inter-motif sequences of *D.*
245 *buzzatii Cenp-C2*, four in *D. seriema Cenp-C1* (two in the Cupin motif and two in inter-motif
246 sequences), and six in inter-motif sequences of *D. seriema Cenp-C2*.

247 Finally, we used clade model C to test for divergent selection among a priori designated lineages.
248 The test reveal evidence of divergent selection acting on *Cid1*, *Cenp-C1* and *Cenp-C2* across almost
249 all the foreground branches, the exception being *D. buzzatii* (Table 4). It is clear that the majority of
250 sites are under negative selection across all lineages, and a small proportion do show signatures of
251 positive selection (data not show); however, there is no obvious pattern of divergent selection across
252 the phylogeny. Unlike the sites-models, clade models freely estimate ω 's for each a priori designated
253 clade and permit sites under positive selection in null models, which could explain the discrepancy
254 among the sites-models and the clade model. Overall, we interpret our data as providing strong
255 support for adaptive evolution at several sites in both the *Cid* and *Cenp-C* paralogs.

256 Our tests revealed that both the *Cid* and *Cenp-C* paralogs show signs of positive selection to some
257 extent. Random-site models revealed that, on average, *Cid5* and *Cenp-C2* show extensive signs of
258 positive selection, which may indicate that these male germline-biased genes possess drive-
259 suppression function. Kursel and Malik (2017) found signs of positive selection in the *Cid3* paralog
260 of the *montium* subgroup and proposed that *Cid3* and *Cid5* could be attenuating deleterious effects of
261 centromere drive due to their male germline-biased expression. Our results of extensive positive
262 selection on both *Cid5* and *Cenp-C2* do support this hypothesis. However, male germline-biased
263 genes are widely known to evolve adaptively as the result of male-male or male-female competition
264 (Ellegren and Parsch 2007; Meisel 2011). On the other hand, branch-site models revealed that
265 different sites of both *Cenp-C1* and *Cenp-C2* show signs of positive selection in *D. buzzatii* and *D.*

266 *seriema*, which may indicate that drive-suppression functions are not restricted to male-biased genes.
267 Either way, molecular genetic data alone cannot reveal the underlying cause of adaptive evolution.
268 What our findings do suggest is that species of the *Drosophila* subgenus likely have a specific inner
269 kinetochore composition that mainly functions in spermatogenesis.

270

271 **Concluding remarks**

272

273 The extensive diversity of kinetochore compositions in eukaryotes poses numerous questions
274 regarding the flexibility of essential cellular functions (van Hooff *et al.* 2017). Is the kinetochore less
275 conserved than other core eukaryotic cellular systems? And if so, why so many core kinetochore
276 proteins are so diverse? Are the variants adaptive to the species? To answer such questions, it is
277 necessary to investigate how a specific kinetochore composition affects specific cellular features and
278 lifestyles. Herein, we showed that *Cid5* and *Cenp-C2* offer such a possibility, as both are inner
279 kinetochore protein variants likely specialized to function mainly in spermatogenesis. Thus, finding
280 out if and how *Cid5* and *Cenp-C2* play a role either in centromere drive suppression or reproductive
281 competition can shed a new light into our understanding of centromere evolution.

282

283 **Materials and methods**

284

285 **Identification of *Cid* and *Cenp-C* orthologs and paralogs in sequenced genomes**

286

287 For most *Drosophila* species, *Cid* and *Cenp-C* coding sequences were obtained from EST data.
288 For *Cenp-C1* of *D. navojoa*, *D. mojavensis*, *D. buzzatii*, *D. seriema* and *D. americana*, *Cenp-C2* of
289 *D. buzzatii*, *D. seriema*, *D. americana* and *D. grimshawi*, *Cid5* of *D. virilis*, and both *Cid5* and *Cid6*
290 of *D. buzzatii* and *D. seriema*, coding sequences were identified by tBLASTx in sequenced genomes.
291 Since *Cid* is encoded by a single exon in *Drosophila*, we selected the entire open reading frame for
292 each *Cid* gene hit, and since *Cenp-C* has multiple introns, we used the Augustus gene prediction
293 algorithm (Stanke and Morgenstern 2005) to identify the coding DNA sequences. For annotated
294 genomes, we recorded the 5' and 3' flanking genes for the *Cid* and *Cenp-C* genes of each species.
295 For genomes that are not annotated, we used the 5' and 3' nucleotide sequences flanking the *Cid* and
296 *Cenp-C* genes as queries to the *D. melanogaster* genome using BLASTn and verified the synteny in
297 accordance to the hits. For the *D. seriema* genome assembly, see Supplementary File S1. All *Cid* and
298 *Cenp-C* coding sequences and their database IDs can be found in Supplementary Files S2 and S3,
299 respectively.

300

301 **Fluorescent *in situ* hybridizations (FISH) on polytene chromosomes**

302

303 Probes for *Cid1/Cid6* were obtained by PCR (see fig. 1A for primer site) from genomic DNA of
304 *D. buzzatii* (strain st-1), *D. seriema* (strain D73C3B), *D. mojavensis* (strain 14021-0248.25) and *D.*
305 *virilis* (strain 15010-1551.51). We cloned the PCR products into the pGEM-T vector (Promega) and
306 sequenced them to confirm identity. Recombinant plasmids were labeled with digoxigenin 11-dUTP
307 by nick translation (Roche Applied Science). FISH on polytene chromosomes was performed as
308 described in Dias *et al.* (2015). The slides were analyzed under an Axio Imager A2 epifluorescence
309 microscope equipped with the AxioCam MRm camera (Zeiss). Images were captured with the
310 AxioVision software (Zeiss) and edited in Adobe Photoshop. Chromosome arms were identified by
311 their morphology (Kuhn *et al.* 1996; González *et al.* 2005; Schaeffer *et al.* 2008).

312

313 **Phylogenetic analyses**

314

315 *Cid* and *Cenp-C* sequences were aligned at the codon level using MUSCLE (Edgar 2004) and
316 refined manually. Subsequently, we generated maximum likelihood phylogenetic trees in MEGA6
317 (Tamura *et al.* 2013) with the GTR substitution model and 1,000 bootstrap replicates for statistical
318 support.

319

320 **Expression analyses**

321

322 RNA-seq data from *D. buzzatii* (Guillén *et al.* 2014), and from *D. virilis* and *D. americana*
323 (BioProject Accession PRJNA376405) were analyzed for the *Cid* and *Cenp-C* expression patterns
324 with Bowtie2 (Langmead and Salzberg 2012), as implemented to the Galaxy server (Afgan *et al.*
325 2016). Mapped reads were normalized by the transcripts per million (TPM) method (Wagner *et al.*
326 2012), and all normalized values < 1 were set to 1 so that $\log_2 \text{TPM} \geq 0$.

327

328 **Positive selection analyses**

329

330 *Cid* and *Cenp-C* alignments and gene trees were used as input into the CodeML NSsites models
331 of PAMLX version 1.3.1 (Xu and Yang 2013). Random-site and branch-site models were used to test
332 for positive selection on particular sites during the evolution of the *Cid* and *Cenp-C* paralogs.
333 Random-site models allow ω to vary among sites but not across lineages; for this analysis, we
334 compared three models that do not allow ω to exceed 1 (M1a, M7 and M8a) to two models that allow
335 $\omega > 1$ (M2a and M8). Branch-site Model A was compared with Model A_{null} to examine whether
336 particular sites evolved under positive selection along a priori specified branches (called foreground

337 branches). Foreground branches were as follow: #1 (*D. arizonae*, *D. mojavensis*); #2 (*D. navojoa*);
338 #3 ((*D. arizonae*, *D. mojavensis*), *D. navojoa*); #4 (*D. buzzatii*); #5 (*D. seriema*); #6 (*D. buzzatii*, *D.*
339 *seriema*). Positively selected sites were classified as those with a Bayes Empirical Bayes posterior
340 probability > 90%. Clade model C (CmC) tests for divergent selection on particular sites among a
341 priori designated lineages. The modified null model of CmC (M2a_rel) assumes that sites fall into
342 three classes: purifying selection ($0 < \omega < 1$); neutral evolution ($\omega = 1$); or positive selection ($\omega > 1$).
343 In CmC, the third site class allows the estimated ω for a site to diverge across foreground branches.
344 Foreground branches were as follow: #1 ((*D. arizonae*, *D. mojavensis*), *D. navojoa*); #2 (*D. buzzatii*,
345 *D. seriema*).

346

347 **Acknowledgments**

348

349 We are grateful to Dr. Maura Helena Manfrin (Univesity of São Paulo) for providing us the *D.*
350 *seriema* strain. This work was supported by a grant from “Fundação de Amparo à Pesquisa do Estado
351 de Minas Gerais” (FAPEMIG) to G.K. (grant number APQ-01563-14).

References

- Afgan E, Baker D, van den Beek M, Blankenberg D, Bouvier D, Čech M, Chilton J, Clements D, Coraor N, Eberhard C, et al. 2016. The Galaxy platform for accessible, reproducible and collaborative biomedical analyses: 2016 update. *Nucleic Acids Res.* 44:W3-W10.
- Casals F, Cáceres M, Manfrin M, González J, Ruiz A. 2005. Molecular Characterization and Chromosomal Distribution of Galileo, Kepler and Newton, Three Foldback Transposable Elements of the *Drosophila buzzatii* Species Complex. *Genetics* 169:2047-2059.
- Clément Y, Tavares R, Marais G. 2006. Does lack of recombination enhance asymmetric evolution among duplicate genes? Insights from the *Drosophila melanogaster* genome. *Gene* 385:89-95.
- Comeron J, Ratnappan R, Bailin S. 2012. The Many Landscapes of Recombination in *Drosophila melanogaster*. *PLoS Genet.* 8:e1002905.
- Dalal Y, Furuyama T, Vermaak D, Henikoff S. 2007. Structure, dynamics, and evolution of centromeric nucleosomes. *Proc Natl Acad Sci USA.* 104:15974-15981.
- Dawe R, Henikoff S. 2006. Centromeres put epigenetics in the driver's seat. *Trends Biochem Sci.* 31:662-669.
- Dias G, Heringer P, Svartman M, Kuhn G. 2015. Helitrons shaping the genomic architecture of *Drosophila*: enrichment of DINE-TR1 in α - and β -heterochromatin, satellite DNA emergence, and piRNA expression. *Chromosome Res.* 23:597-613.
- Edgar R. 2004. MUSCLE: multiple sequence alignment with high accuracy and high throughput. *Nucleic Acids Res.* 32:1792-1797.
- Erhardt S, Mellone B, Betts C, Zhang W, Karpen G, Straight A. 2008. Genome-wide analysis reveals a cell cycle-dependent mechanism controlling centromere propagation. *J Cell Biol.* 183:805-818.
- Finseth F, Dong Y, Saunders A, Fishman L. 2015. Duplication and Adaptive Evolution of a Key Centromeric Protein in *Mimulus*, a Genus with Female Meiotic Drive. *Mol Biol Evol.* 32:2694-2706.
- Fishman L, Saunders A. 2008. Centromere-Associated Female Meiotic Drive Entails Male Fitness Costs in Monkeyflowers. *Science* 322:1559-1562.
- Gonzalez J, Nefedov M, Bosdet I, Casals F, Calvete O, Delprat A, Shin H, Chiu R, Mathewson C, Wye N, et al. 2005. A BAC-based physical map of the *Drosophila buzzatii* genome. *Genome Res.* 15:885-889.
- Guillén Y, Rius N, Delprat A, Williford A, Muyas F, Puig M, Casillas S, Ràmia M, Egea R, Negre B, et al. 2014. Genomics of Ecological Adaptation in Cactophilic *Drosophila*. *Genome Biol Evol.* 7:349-366.

- Heeger S, Leismann O, Schittenhelm R, Schraidt O, Heidmann S, Lehner C. 2005. Genetic interactions of separate regulatory subunits reveal the diverged *Drosophila* Cenp-C homolog. *Genes Dev.* 19:2041-2053.
- Henikoff S, Ahmad K, Malik H. 2001. The Centromere Paradox: Stable Inheritance with Rapidly Evolving DNA. *Science* 293:1098-1102.
- Henikoff S, Ahmad K, Platero J, van Steensel B. 2000. Heterochromatic deposition of centromeric histone H3-like proteins. *Proc Natl Acad Sci USA* 97:716-721.
- Iwata-Otsubo A, Dawicki-McKenna JM, Akera T, Falk SJ, Chmátal L, Yang K, Sullivan BA, Schultz RM, Lampson MA, Black BE. 2017. Expanded Satellite Repeats Amplify a Discrete CENP-A Nucleosome Assembly Site on Chromosomes that Drive in Female Meiosis. *Curr Biology* doi:10.1016/j.cub.2017.06.069
- Kohany O, Gentles A, Hankus L, Jurka J. 2006. Annotation, submission and screening of repetitive elements in Repbase: RepbaseSubmitter and Censor. *BMC Bioinformatics* 7:474.
- Kuhn G, Ruiz A, Alves M, Sene F. 1996. The metaphase and polytene chromosomes of *Drosophila seriema* (repleta group; mulleri subgroup). *Brazilian Journal of Genetics* 19:209–216.
- Kursel L, Malik H. 2017. Recurrent Gene Duplication Leads to Diverse Repertoires of Centromeric Histones in *Drosophila* Species. *Mol Biol Evol.* doi: 10.1093/molbev/msx091.
- Langmead B, Salzberg S. 2012. Fast gapped-read alignment with Bowtie 2. *Nat Methods* 9:357-359.
- Liu Y, Petrovic A, Rombaut P, Mosalaganti S, Keller J, Raunser S, Herzog F, Musacchio A. 2016. Insights from the reconstitution of the divergent outer kinetochore of *Drosophila melanogaster*. *Open Biol.* 6:150236.
- Malik H, Henikoff S. 2009. Major Evolutionary Transitions in Centromere Complexity. *Cell* 138:1067-1082.
- Nambiar M, Smith G. 2016. Repression of harmful meiotic recombination in centromeric regions. *Semin Cell Dev Biol.* 54:188-197.
- Oliveira D, Almeida F, O’Grady P, Armella M, DeSalle R, Etges W. 2012. Monophyly, divergence times, and evolution of host plant use inferred from a revised phylogeny of the *Drosophila* repleta species group. *Mol Phylogenet Evol.* 64:533-544.
- Orr B, Sunkel C. 2011. *Drosophila* CENP-C is essential for centromere identity. *Chromosoma* 120:83-96.
- Pimpinelli S, Berloco M, Fanti L, Dimitri P, Bonaccorsi s, Marchetti E, Caizzi R, Caggese C, Gatti M. 1995. Transposable elements are stable structural components of *Drosophila melanogaster* heterochromatin. *Proc Natl Acad Sci USA* 92:3804-3808.

- Plohl M, Luchetti A, Meštrović N, Mantovani B. 2008. Satellite DNAs between selfishness and functionality: Structure, genomics and evolution of tandem repeats in centromeric (hetero)chromatin. *Gene* 409:72-82.
- Przewloka M, Venkei Z, Bolanos-Garcia VM, Debski J, Dadlez M, Glover DM. 2011. CENP-C is a Structural Platform for Kinetochores Assembly. *Curr Biol.* 21:399-405.
- Rius N, Guillén Y, Delprat A, Kapusta A, Feschotte C, Ruiz A. 2016. Exploration of the *Drosophila buzzatii* transposable element content suggests underestimation of repeats in *Drosophila* genomes. *BMC Genomics* 10:17-344.
- Ross B, Malik H. 2014. Genetic Conflicts: Stronger Centromeres Win Tug-of-War in Female Meiosis. *Current Biology* 24:R966-R968.
- Russo C, Mello B, Frazão A, Voloch C. 2013. Phylogenetic analysis and a time tree for a large drosophilid data set (Diptera: Drosophilidae). *Zoological Journal of the Linnean Society* 169:765-775.
- Rutkowska J, Badyaev A. 2008. Meiotic drive and sex determination: molecular and cytological mechanisms of sex ratio adjustment in birds. *Philosophical Transactions of the Royal Society B: Biological Sciences* 363:1675-1686.
- Schaeffer S, Bhutkar A, McAllister B, Matsuda M, Matzkin L, O'Grady P, Rohde C, Valente V, Aguade M, Anderson W, et al. 2008. Polytene Chromosomal Maps of 11 *Drosophila* Species: The Order of Genomic Scaffolds Inferred From Genetic and Physical Maps. *Genetics* 179:1601-1655.
- Schittenhelm RB, Althoff F, Heidmann S, Lehner C. 2010. Detrimental incorporation of excess Cenp-A/Cid and Cenp-C into *Drosophila* centromeres is prevented by limiting amounts of the bridging factor Cal1. *Journal of Cell Science* 123:3768-3779.
- Schuh M, Lehner CF, Heidmann S. 2007. Incorporation of *Drosophila* CID/Cenp-A and CENP-C into centromeres during early embryonic anaphase. *Curr Biol.* 17:237-243.
- Stanke M, Morgenstern B. 2005. AUGUSTUS: a web server for gene prediction in eukaryotes that allows user-defined constraints. *Nucleic Acids Res.* 33:W465-W467.
- Talbert P, Bryson T, Henikoff S. 2004. Adaptive evolution of centromere proteins in plants and animals. *J Biol.* 3:18.
- Tamura K, Stecher G, Peterson D, Filipinski A, Kumar S. 2013. MEGA6: Molecular Evolutionary Genetics Analysis Version 6.0. *Mol Biol Evol.* 30:2725-2729.
- van Hooff J, Tromer E, van Wijk LM, Snel B, Kops G. 2017. Evolutionary dynamics of the kinetochore network in eukaryotes as revealed by comparative genomics. *EMBO reports* doi:10.15252/embr.201744102

- Wagner G, Kin K, Lynch V. 2012. Measurement of mRNA abundance using RNA-seq data: RPKM measure is inconsistent among samples. *Theory Biosci.* 131:281-285.
- Xu B, Yang Z. 2013. PAMLX: a graphical user interface for PAML. *Mol Biol Evol.* 30:2723-2724
- Zhang Z, Kishino H. 2004. Genomic Background Predicts the Fate of Duplicated Genes: Evidence From the Yeast Genome. *Genetics* 166:1995-1999.

Tables

Table 1. Genetic distances between the *Cenp-C* paralogs.

	<i>Sophophora</i> Cenp-C1	<i>Drosophila</i> Cenp-C1	<i>Drosophila</i> Cenp-C2	Overall
R-rich	0.304 (0.254)	0.435 (0.593)	0.267 (0.244)	0.463 (0.513)
DH	0.292 (0.295)	0.304 (0.380)	0.283 (0.316)	0.394 (0.445)
AT1	0.453 (0.505)	-	-	-
NLS	0.281 (0.203)	0.386 (0.443)	0.284 (0.275)	0.402 (0.413)
CenH3	0.316 (0.353)	0.237 (0.232)	0.254 (0.266)	0.352 (0.371)
AT2	0.421 (0.530)	-	0.301 (0.390)	0.419 (0.498)
Cupin	0.334 (0.402)	0.294 (0.372)	0.236 (0.283)	0.422 (0.517)
Full-sequence	0.404 (0.487)	0.375 (0.484)	0.363 (0.458)	0.511 (0.634)

Note – Values refer to distances between coding DNA sequences (values between brackets refer to amino acids distances).

Table 2. Summary of random-site models for positive selection performed on each *Cid* and *Cenp-C* paralog.

	Alignment length (#nts)	M1a vs. M2a	M7 vs. M8	M8a vs. M8
<i>Cid1/Cid6</i>	609	$P = 1$	$P = 1$	$P = 0.982$
<i>Cid5</i>	600	$P = 0.099$	$P = 0.069$	$P = 0.025$
<i>Cenp-C1</i>	3,492	$P = 0.496$	$P = 0.163$	$P = 0.210$
<i>Cenp-C2</i>	3,696	$P = 0.194$	$P = 0.005$	$P = 0.068$

Table 3. Summary of branch-site models for positive selection performed on each *Cid* and *Cenp-C* paralog.

	MA vs. MAnull					
	#1	#2	#3	#4	#5	#6
<i>Cid1</i>	$P = 1$	$P = 1,34E-06$	$P = 1$	$P = 1$	$P = 0.251$	$P = 1$
<i>Cid5</i>	$P = 0.215$	$P = 1$	$P = 1$	$P = 1$	$P = 1$	$P = 1$
<i>Cenp-C1</i>	$P = 1$	$P = 0.303$	$P = 1$	$P = 0.0328$	$P = 1,08E-04$	$P = 1$
<i>Cenp-C2</i>	$P = 1$	$P = 1,64E-05$	$P = 0.139$	$P = 0.041$	$P = 0.03$	$P = 0.28$

Note – Foreground branches are as follow: #1 (*D. arizonae*, *D. mojavensis*); #2 (*D. navojoa*); #3 ((*D. arizonae*, *D. mojavensis*), *D. navojoa*); #4 (*D. buzzatii*); #5 (*D. seriema*); #6 (*D. buzzatii*, *D. seriema*).

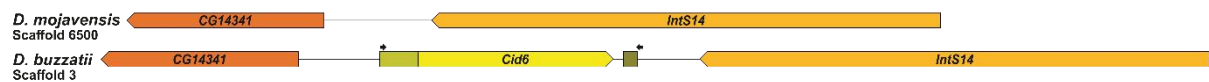
Table 4. Summary of the clade model for divergent selection performed on each *Cid* and *Cenp-C* paralog.

	CmC vs. M2a_rel					
	#1	#2	#3	#4	#5	#6
<i>Cid1</i>	$P = 0.0575$	$P = 0.048$	$P = 0.016$	$P = 0.129$	$P = 0.009$	$P = 0.022$
<i>Cid5</i>	$P = 0.180$	$P = 0.536$	$P = 0.309$	$P = 0.159$	$P = 0.918$	$P = 0.498$
<i>Cenp-C1</i>	$P = 0.0006$	$P = 0.363$	$P = 0.039$	$P = 0.072$	$P = 0.108$	$P = 0.044$
<i>Cenp-C2</i>	$P = 0.00005$	$P = 0.005$	$P = 0.068$	$P = 0.227$	$P = 0.011$	$P = 1$

Note – Foreground branches are as follow: #1 (*D. arizonae*, *D. mojavensis*); #2 (*D. navojoa*); #3 ((*D. arizonae*, *D. mojavensis*), *D. navojoa*); #4 (*D. buzzatii*); #5 (*D. seriema*); #6 (*D. buzzatii*, *D. seriema*).

Figures

Cid6 locus – Muller element B (chromosome 3)



Cid1 locus – Muller element C (chromosome 5)

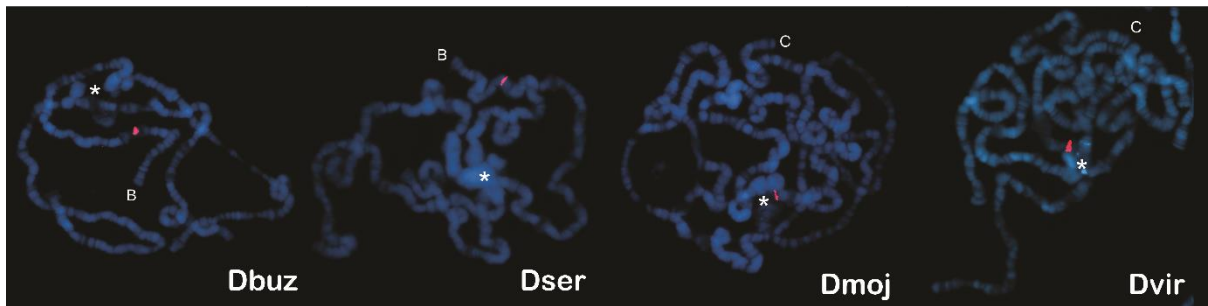
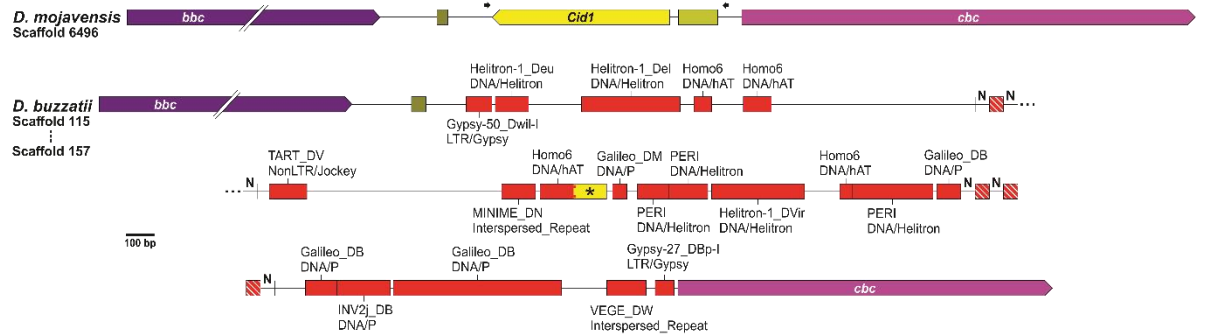


Figure 1. *Cid1* degenerated after the inter-chromosomal duplication event giving rise to *Cid6*. (Upper panel) Comparison between the *Cid1* and *Cid6* loci of *D. buzzatii* and the corresponding regions of *D. mojavensis*. The black asterisk indicates a fragment of *Cid1*, ‘N’ indicates unidentified nucleotides, red boxes indicate transposable elements, and arrows indicate primers used for the fluorescent *in situ* hybridization (FISH) experiments. (Lower panel) FISH on polytene chromosomes of *D. buzzatii* (Dbuz) and *D. seriema* (Dser) using *Cid6* probes, and of the closely related *D. mojavensis* (Dmoj) and the outgroup *D. virilis* (Dvir) using *Cid1* probes. The chromosome arm in which the *Cid* probe hybridized (red signal) is indicated by a letter representing the corresponding Muller element. The chromocenter, a region in which all centromeres bundle together, is indicated by a white asterisk. (Note: the chromocenter of *D. buzzatii* and *D. mojavensis* ruptured during the fixation step).

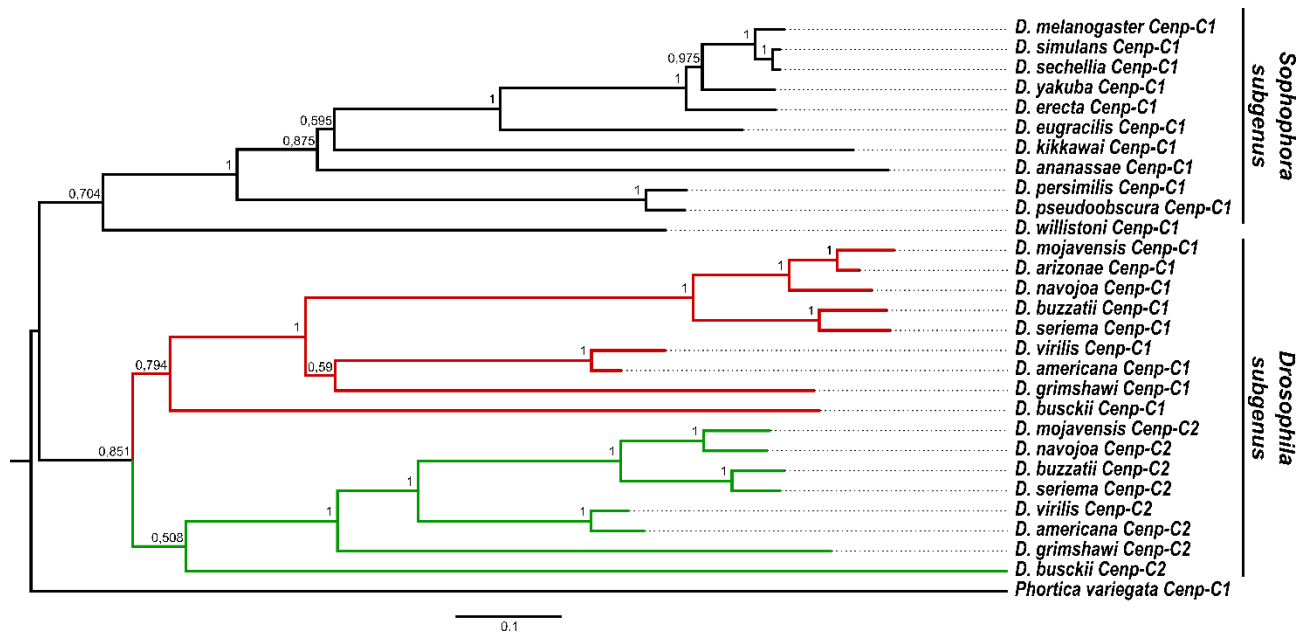


Figure 2. *Cnp-C1* duplicated in the lineage that gave rise to species of the *Drosophila* subgenus. Maximum likelihood tree of the *Cnp-C1* and *Cnp-C2* paralogs. Red and green branches respectively correspond to *Cnp-C1* and *Cnp-C2* sequences from species of the *Drosophila* subgenus. Bootstrap values are shown in each node. Scale bar represents number of substitutions per site.

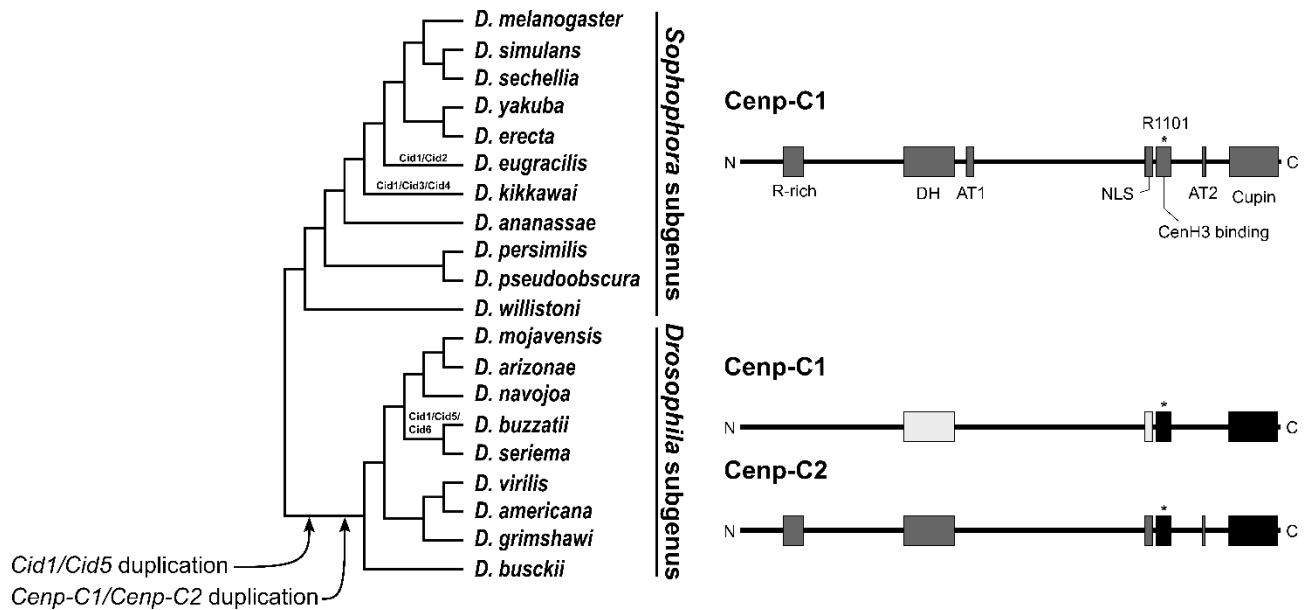


Figure 3. Some Cenp-C motifs are alternatively conserved between Cenp-C1 and Cenp-C2. Both *Cid* and *Cenp-C* genes were duplicated in the lineage that gave rise to species of the *Drosophila* subgenus, as indicated in the species tree. Moreover, *Cid1* was also duplicated in *D. eugracilis*, the *montium* subgroup (which includes *D. kikkawai*), and the *buzzatii* species cluster, the new paralogs of which are indicated at their respective branches. After the *Cenp-C* duplication, some functional motifs were alternatively conserved between the paralogs, as indicated at the right half of the image. High amino acids identity is indicated by the same color shade. Motifs are as follow: R-rich, arginine-rich; DH, drosophilid Cenp-C homology; AT1, AT hook 1; NLS, nuclear localization signal; CenH3 binding, also known as Cenp-C motif; AT2, AT hook 2; Cupin, a dimerization domain near the C-terminal region. The asterisk in the CenH3 binding motif indicates the corresponding R1101 of *D. melanogaster*, which is crucial for the centromere localization of Cenp-C1.

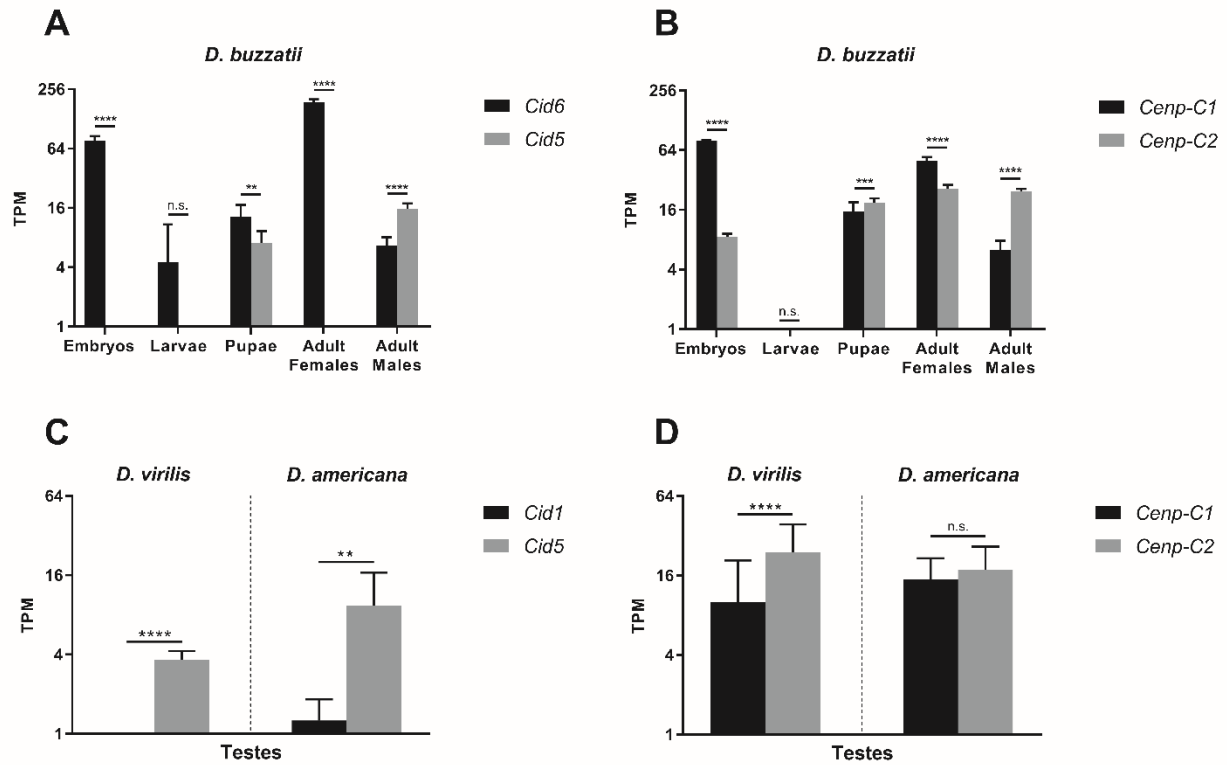


Figure 4. *Cid5* and *Cenp-C2* are male germline-biased. *Cid* and *Cenp-C* expression patterns in *D. buzzatii* (A and B) and *D. virilis* and *D. americana* (C and D). Data are presented as mean \pm 95% confidence interval and analyzed by one-way ANOVA (A and B) and Student's t-test (C and D): n.s., not significant; * $P \leq 0.05$; ** $P \leq 0.01$; *** $P \leq 0.001$; **** $P \leq 0.0001$. TPM, transcripts per million.



Supplementary Figure S1. Some Cenp-C motifs are alternatively conserved between Cenp-C1 and Cenp-C2. (A) Schematic representation of the motif structure of *D. melanogaster* Cenp-C1. (B) Logo representations for each motif of the *Drosophila* subgenus Cenp-C1 (C1) and Cenp-C2 (C2). Motifs are as follow: R-rich, arginine-rich; DH, drosophilid Cenp-C homology; AT1, AT hook 1; NLS, nuclear localization signal; CenH3 binding, also known as Cenp-C motif; AT2, AT hook 2; Cupin, a dimerization domain near the C-terminal region. The asterisk in the CenH3 binding motif indicates the corresponding R1101 of *D. melanogaster*, which is crucial for the centromere localization of Cenp-C1.